

AN APPROXIMATE ANALYTICAL SOLUTION OF A 4-DOF VARIABLE-LENGTH PENDULUM MODEL

GODIYA YAKUBU, PAWEŁ OLEJNIK

Lodz University of Technology, Department of Automation, Biomechanics and Mechatronics, Łódź, Poland

e-mail: godiesluv59@gmail.com; pawel.olejnik@p.lodz.pl

In this work, we employ the multiple scale method to introduce a novel analytical solution for an extended four-degrees-of-freedom dynamical system modeled on a swinging Atwood machine. We provide a methodology for obtaining the asymptotic solution up to the second-order approximation for both the swinging and modified swinging Atwood machine, demonstrating its solvability through the multiple scale approach. Subsequently, we present a comparative analysis of time histories between numerical and analytical solutions. These analytical solutions are of particular significance in applied mechanics, given their practical applications in parametric dynamical models grounded in the pendulum concept.

Keywords: analytical solutions, asymptotic solutions, swinging Atwood machine, multiple scale method

1. Introduction

Analytical solutions find extensive applications across physics, engineering, and mathematics. Their versatility allows for simulating a wide range of systems, from elementary pendulums to intricate electromagnetic fields. Furthermore, these solutions prove invaluable in validating numerical methods, offering a reliable benchmark for precise comparison and assessment.

Drawing from the existing body of literature on variable-length pendulums (Yakubu *et al.*, 2022), it becomes apparent that the modeling and analysis of parametric dynamical models for such pendulums can be intricate and demanding. The applications of such pendulums in mechanical and mechatronic systems provide a compelling motivation for undertaking research in this area, and they have a strong presence in both theoretical and practical engineering applications.

The multiple scale approach is a widely utilized technique for finding analytical solutions of dynamical systems, as evidenced by various authors in the following references: Abady *et al.* (2022), Abohamer *et al.* (2023a,b), Awrejcewicz *et al.* (2022), Starosta *et al.* (2017), Manafian and Allahverdiyeva (2022). A recent publication by Prokopenya (2021) tackled the problem of finding solutions to the equations of motion of swinging Atwood machine, a system comprised of two equal masses that oscillate and are in a state of dynamic equilibrium. The author derived the system differential equations of motion and computed them in the form of a power series with a small parameter.

Obtaining an analytical solution for novel 4-degrees of freedom (4-DOF) modified swinging Atwood machine (SAM) holds immense significance. This is primarily due to its ability to provide fast, stable, and precise solutions that can be readily understood and explicitly expressed due to its parameter dependencies (Manafian and Allahverdiyeva, 2022; Seadawy and Manafian, 2018; Starosta *et al.*, 2017).

To explore the potentially intricate dynamics of a variable-length pendulum in a range of engineering and mechatronic systems, we introduce a novel 4-DOF variable-length pendulum model. This pendulum is analytically solved, and a comparative analysis is performed to identify

correlative features between analytical and numerical solutions, thus verifying the accuracy of the computational model. The primary objective of this analysis is to uncover the system internal structure by identifying all the existing resonances. The analytical solution presented allows for the resolution of resonance issues by making appropriate adjustments to the forcing term when the model is applied in engineering and mechatronic systems. This ensures that the pendulum operates optimally in various practical applications.

In this paper, we utilized the multiple scale method, which allowed us to derive an asymptotic solution up to the second-order approximation of the SAM. The objective was to gain insight into applying the same technique for analytically solving the novel modified SAM with 4-DOF. Accordingly, we applied the same multiple scale method and derived the analytical solution for the modified SAM.

Before delving into procedures for finding solutions, the main assumptions are presented in Section 1.1. This approach ensures that the reader has a clear understanding of the underlying assumptions that are used in developing the analytical solution. Furthermore, by establishing the key assumptions upfront, the subsequent steps in the solution-finding process are grounded in a well-defined set of criteria. Therefore, by clearly stating the main assumptions at the outset, we can ensure that the subsequent analysis is rigorous, transparent, and logically consistent.

1.1. Main assumptions

To approximate the solution to the differential equation, a series expansion based on powers of a small parameter is employed (Awrejcewicz *et al.*, 2022). Each term in the series represents a distinct time or length scale (Abohamer *et al.*, 2023b; Awrejcewicz *et al.*, 2022). In order to streamline the resulting equations, the higher-order terms associated with the small parameter are neglected.

The precision of a multiple scale solution relies on the small parameter size and the number of terms incorporated in the series expansion. Generally, a more accurate solution is achieved when more terms are added in the expansion (Awrejcewicz *et al.*, 2022; Nayfeh, 2005). However, it is important to acknowledge that despite the potential for increased accuracy with more terms, the complexity of the equations often requires limiting Taylor's series expansion to the inceptive terms only.

Considering the assumptions mentioned earlier, we have neglected the impact of frictional forces in the model equations. To make the system suitable for investigation, we transformed the equations of motion into a dimensionless form to make it solvable using multiple scales. In doing so, we introduced specific dimensionless terms. Furthermore, we offset the time-dependent variables $x(t)$ and $\dot{\phi}(t)$ in the SAM model, and $x_1(t)$ and $\dot{\phi}_1(t)$ in the modified SAM model by an independent variable designated by λ .

2. The swinging Atwood machine

The SAM is a classical mechanics concept that can aid in comprehending the variable-length pendulum. In this particular system, the pendulum body oscillates within a two-dimensional plane, displaying a diverse range of dynamic behavior while remaining disconnected from another mass known as the counterweight (Elmandouh, 2016; Prokopeny, 2017; Tuffillaro, 1985). In the initial approach, the two bodies are linked by an unyielding weightless string suspended on two pulleys devoid of friction (Tuffillaro, 1994), as demonstrated in Fig. 1a.

The behavior of the SAM can be described by employing concepts of circular motion, centripetal force, and energy conservation. The tension in the string creates the centripetal force which enables the pendulum, mass m , to move horizontally to follow a circular trajectory, and the counterweight of mass M to move vertically, solely influenced by the force of gravity only

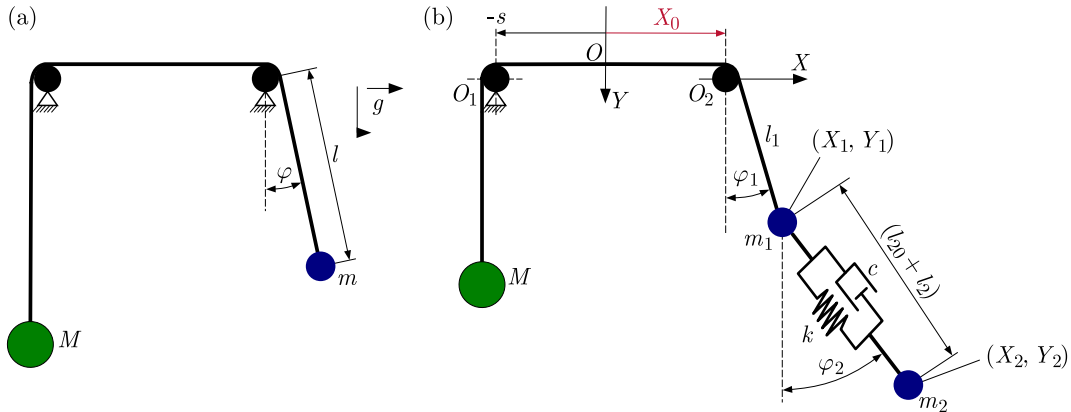


Fig. 1. (a) The initial physical model of the 2-DOF SAM: M – counterweight, m – pendulum body; (b) the proposed original Modified SAM

(Elmandouh, 2016; Tuffillaro *et al.*, 1988). By analyzing motion of this system, various physical phenomena can be explored, such as conservation of angular momentum and the impact of centripetal force on object motion. Due to the pendulum reactive centrifugal force opposing the weight of the counterweight mass M , the dynamic response of the system can exhibit characteristics such as singularity or non-singularity, chaos or quasi-periodicity, boundedness or unboundedness, and even discontinuity (Casasayas *et al.*, 1990; Tuffillaro, 1986; Nunes *et al.*, 1995; Pujol *et al.*, 2010; Yehia, 2006).

2.1. Equations of motion

The system being examined possesses two degrees of freedom. First, by utilizing the Lagrangian L , one can deduce the equation of motion (Elmandouh, 2016) for T and U , which respectively denote the kinetic and potential energy. The equations of motion for the SAM as described by Prokopenya (2021), Elmandouh (2016), Tuffillaro *et al.* (1988), Tuffillaro (1994), Casasayas *et al.* (1990), Nunes *et al.* (1995), Pujol *et al.* (2010), Yehia (2006), Tuffillaro (1985) are presented below.

Upon considering the initial state-space variable, we observe that the two ordinary differential equations (ODEs) encompass the dynamics along the two independent degrees of freedom, i.e., $\varphi(t)$ and $l(t)$

$$\frac{\partial L}{\partial \varphi} = \frac{d}{dt} \left(\frac{\partial L}{\partial \dot{\varphi}} \right) \quad \frac{\partial L}{\partial l} = \frac{d}{dt} \left(\frac{\partial L}{\partial \dot{l}} \right) \quad (2.1)$$

Based on the presented model illustrated in Fig. 1a, we express the following

$$T = \frac{1}{2} M \dot{l}^2(t) + \frac{1}{2} m [\dot{l}^2(t) + l^2(t) \dot{\varphi}^2(t)] \quad U = Mgl(t) - mgl(t) \cos \varphi(t) \quad (2.2)$$

where M is the non-swinging mass, m – pendulum mass as it swings, $l(t)$ – distance from the pivot point to the center of the swinging pendulum body.

We determine the Lagrangian as $L = T - U$, i.e.

$$L = \frac{1}{2} M \dot{l}^2(t) + \frac{1}{2} m [\dot{l}^2(t) + l^2(t) \dot{\varphi}^2(t)] - Mgl(t) + mgl(t) \cos \varphi(t) \quad (2.3)$$

Given that the Hamiltonian $H = T + U$ is defined in terms of the canonical momenta p_l and p_φ , we obtain the following

$$H = \frac{p_l^2}{2(M+m)} + \frac{p_\varphi^2}{2ml^2(t)} + Mgl(t) - mgl \cos \varphi(t) \quad (2.4)$$

where: $p_l = (M+m)\dot{l}(t)$, $p_\varphi = ml^2(t)\dot{\varphi}(t)$.

The equations governing dynamical behavior in the state-space variables φ and l can be obtained based on the aforementioned assumptions

$$\begin{aligned} l(t)\ddot{\varphi}(t) + 2\dot{l}(t)\dot{\varphi}(t) + g \sin \varphi(t) &= 0 \\ ml(t)\dot{\varphi}^2(t) - Mg + mg \cos \varphi(t) &= (M + m)\ddot{l}(t) \end{aligned} \quad (2.5)$$

Taking into account the mass ratio $\mu_m = M/m$, then Eq. (2.5)₂ becomes

$$(\mu_m + 1)\ddot{l}(t) - l(t)\dot{\varphi}^2(t) + g[\mu_m - \cos \varphi(t)] = 0 \quad (2.6)$$

In order to find the solution of the systems using the MSM method, the following parameters are employed

$$\begin{aligned} \omega_2^2 &= \frac{g}{l} & \omega_4^2 &= \frac{\omega_2^2}{\omega_1^2} & \sigma_1 &= \frac{\lambda^3}{(\mu + 1)\omega_1^2} + \frac{\mu\omega_4^2}{\mu + 1} - \frac{\omega_4^2}{\mu + 1} \\ \sigma_2 &= \frac{\lambda^2}{(\mu + 1)\omega_1^2} & \sigma_3 &= \frac{\omega_4^2}{3(\mu + 1)} & \zeta_5 &= \frac{1}{\lambda} & \sigma_4 &= \frac{2\lambda^2}{(\mu + 1)\omega_1} \\ \sigma_5 &= \frac{2\lambda}{(\mu + 1)\omega_1} & \sigma_6 &= -\frac{\lambda}{\mu + 1} & \sigma_7 &= \frac{1}{\mu + 1} & \zeta_1 &= \omega_4^2 \\ \zeta_2 &= \frac{\omega_4^2}{6} & \zeta_3 &= \frac{2}{\omega_1} & \zeta_4 &= \frac{2}{\lambda} \end{aligned} \quad (2.7)$$

Moreover, we employed the Taylor series to incorporate an additional approximation. In particular, we considered only the first term of Taylor's expansion, resulting in the following expression

$$\sin \phi(t) = \phi(t) - \frac{\phi^3(t)}{6} \quad \cos \phi(t) = 1 - \frac{\phi^2(t)}{2} \quad (2.8)$$

By utilizing the parameters specified in Eqs. (2.7) and (2.8), Eqs. (2.5) are transformed into their final dimensionless form, which can be expressed as follows

$$\begin{aligned} \sigma_1 + \sigma_2 x(\tau) + \sigma_3 \phi(\tau)^2 + \sigma_4 \dot{\phi}_1(\tau) + \sigma_5 x(\tau)\dot{\phi}(\tau) + \sigma_6 \dot{\phi}(\tau)^2 + \sigma_7 x(\tau)\dot{\phi}(\tau)^2 + \ddot{x}(\tau) &= 0 \\ \zeta_1 \phi(\tau) - \zeta_2 \phi(\tau)^3 + \zeta_3 \dot{x}(\tau) + \zeta_4 \dot{\phi}(\tau)\dot{x}(\tau) + \ddot{\phi}(\tau) + \zeta_5 x(\tau)\ddot{\phi}(\tau) &= 0 \end{aligned} \quad (2.9)$$

where τ represents the dimensionless time, $x(\tau)$ and $\phi(\tau)$ are dimensionless forms of $l(t)$ and $\varphi(t)$, respectively. ω_1 is first associated with $\dot{\phi}(\tau)$, then λ is introduced into both $x(\tau)$ and $\dot{\phi}(\tau)$ as a way to partially linearize the nonlinear terms ensuring that they appear in the equation where they should be. This effectively helps in decoupling the left-hand side of the approximate solution using the multiple scale method.

2.2. The multiple scale approach technique

In this Section, we apply the multiple scale approach to obtain asymptotic solutions for the equations mentioned in Eqs. (2.9). In accordance with the multiple scale technique, we examine the dynamics of the systems under consideration within a close range around their static equilibrium position (Abohmer *et al.*, 2023a; Awrejcewicz *et al.*, 2022). In order to characterize the amplitudes of oscillations within this region, we introduce a small parameter denoted as $0 < \varepsilon \ll 1$, which allows us to establish the following relationship

$$x(\tau) = \varepsilon \alpha(\tau : \varepsilon) \quad \phi(\tau) = \varepsilon \gamma(\tau : \varepsilon) \quad (2.10)$$

This enabled us to consider the following approximations

$$\begin{aligned} \sigma_1 &= \varepsilon^2 \tilde{\sigma}_1 & \sigma_4 &= \varepsilon^1 \tilde{\sigma}_4 & \sigma_7 &= \varepsilon^{-1} \tilde{\sigma}_7 \\ \zeta_2 &= \varepsilon^{-1} \tilde{\zeta}_2 & \zeta_3 &= \varepsilon \tilde{\zeta}_3 & \zeta_5 &= \varepsilon^0 \tilde{\zeta}_5 \end{aligned} \quad (2.11)$$

where ε is a parameter used for bookkeeping, having no impact on the computation and not appearing in the final approximate solution. Its purpose is to ensure that all other terms from the original equations are included in the solution process. We assume that ε is small enough to avoid computational errors.

In accordance with the multiple scale approach, the time-dependent variable $x(\tau)$, and $\phi(\tau)$ can be considered as a power series of ε

$$x(\tau) = \sum_{k=1}^2 \varepsilon^k x_{,k}(\tau_0, \tau_1) + O(\varepsilon^k) \quad \phi(\tau) = \sum_{k=1}^2 \varepsilon^k \phi_{,k}(\tau_0, \tau_1) + O(\varepsilon^k) \quad (2.12)$$

where $\tau_n = \varepsilon^n \tau (n = 0, 1)$ with τ_0 being the fastest and τ_1 being the slowest.

To convert the derivatives with respect to τ to the new time scales τ_n , the following operators are employed

$$\frac{d}{d\tau} = \frac{\partial}{\partial \tau_0} + \varepsilon \frac{\partial}{\partial \tau_1} \quad \frac{d^2}{d\tau^2} = \frac{\partial^2}{\partial \tau_0^2} + 2\varepsilon \frac{\partial^2}{\partial \tau_0 \partial \tau_1} + O(\varepsilon^2) \quad (2.13)$$

It is worth noting that these operators neglect terms of $O(\varepsilon^2)$ and higher orders. To obtain the partial differential equation (PDE) groups corresponding to different powers of ε , we substitute equations (2.10)-(2.13) into the dimensionless form of governing equations (2.9). This procedure leads to derivation of the preceding four linear PDEs. Based on the perturbation parameter ε , the splitting method is employed for obtaining these PDEs (Awrejcewicz *et al.*, 2022). These equations are the orders of ε and ε^2 :

— first-order equations (coefficient 1 at ε^1)

$$\frac{\partial^2 \alpha_1}{\partial \tau_0^2} + \sigma_2 \alpha_1 = 0 \quad \frac{\partial^2 \gamma_1}{\partial \tau_0^2} + \zeta_1 \gamma_1 = 0 \quad (2.14)$$

— second-order equations (coefficient 2 at ε^2)

$$\begin{aligned} & \tilde{\sigma}_1 + \sigma_2 \alpha_2 + \sigma_3 \gamma_1^2 + \tilde{\sigma}_4 \gamma_1 \frac{\partial \gamma_1}{\partial \tau_0} + \sigma_5 \alpha_1 \gamma_1 \frac{\partial \gamma_1}{\partial \tau_0} + \sigma_6 \left(\frac{\partial \gamma_1}{\partial \tau_0} \right)^2 \\ & + \tilde{\sigma}_7 \alpha_1 \left(\frac{\partial \gamma_1}{\partial \tau_0} \right)^2 + 2 \frac{\partial^2 \alpha_1}{\partial \tau_0 \partial \tau_1} + \frac{\partial^2 \alpha_2}{\partial \tau_0^2} = 0 \\ & \zeta_1 \gamma_2 - \tilde{\zeta}_2 \gamma_1^3 + \tilde{\zeta}_3 \frac{\partial \alpha_1}{\partial \tau_0} + \zeta_4 \frac{\partial \alpha_1}{\partial \tau_0} \frac{\partial \gamma_1}{\partial \tau_0} + 2 \frac{\partial^2 \gamma_1}{\partial \tau_0 \partial \tau_1} + \tilde{\zeta}_5 \alpha_1 \frac{\partial^2 \gamma_1}{\partial \tau_0^2} + \frac{\partial^2 \gamma_2}{\partial \tau_0^2} = 0 \end{aligned} \quad (2.15)$$

where α_1 and γ_1 represent the solution of the first-order approximations of the time-dependent variables $x(\tau)$ and $\phi_1(\tau)$, respectively. Also, α_2 and γ_2 are the solution of the second-order approximations of the time-dependent variables $x(\tau)$ and $\phi_1(\tau)$. Meanwhile, α and γ will represent the respective general solutions of the time-dependent variables.

The solutions to Eqs. (2.15) are required to be solved in a specific order. Notably, the solutions obtained from the first group hold significant importance. Therefore, our initial emphasis lies in acquiring the general solutions to Eq. (2.14). The resulting established solutions are presented as follows

$$\alpha_1 = e^{i\sigma_2 \tau_0} B_1(\tau_1) + e^{-i\sigma_2 \tau_0} \tilde{B}_1(\tau_1) \quad \gamma_1 = e^{i\zeta_1 \tau_0} B_3(\tau_1) + e^{-i\zeta_1 \tau_0} \tilde{B}_3(\tau_1) \quad (2.16)$$

Consequently, by substituting solutions (2.16) into the second group of PDEs (2.15), we obtain the following second-order solutions with B_i and \tilde{B}_i being τ_1 dependent, where $i = 1, 2$

$$\begin{aligned} \alpha_2 = & -\frac{-2\zeta_1^2\sigma_6B_2(\tau_1)\tilde{B}_2(\tau_1) - 2\sigma_3B_2(\tau_1)\tilde{B}_2(\tau_1) + \tilde{\sigma}_1}{\sigma_2^2} + \frac{i\sigma_5B_1(\tau_1)B_2(\tau_1)e^{i\tau_0(\zeta_1+\sigma_2)}}{\zeta_1 + 2\sigma_2} \\ & - \frac{e^{2i\zeta_1\tau_0}[\zeta_1^2\sigma_6B_2(\tau_1)^2 - \sigma_3B_2(\tau_1)^2]}{(2\zeta_1 - \sigma_2)(2\zeta_1 + \sigma_2)} + \frac{i\zeta_1\tilde{\sigma}_4B_2(\tau_1)e^{i\zeta_1\tau_0}}{(\zeta_1 - \sigma_2)(\zeta_1 + \sigma_2)} - \frac{\zeta_1\tilde{\sigma}_7B_1(\tau_1)B_2(\tau_1)^2e^{i\tau_0(2\zeta_1+\sigma_2)}}{4(\zeta_1 + \sigma_2)} \\ & + \frac{i\sigma_5B_2(\tau_1)\tilde{B}_1(\tau_1)e^{i\tau_0(\zeta_1-\sigma_2)}}{\zeta_1 - 2\sigma_2} - \frac{\zeta_1\tilde{\sigma}_7B_2(\tau_1)^2\tilde{B}_1(\tau_1)e^{i\tau_0(2\zeta_1-\sigma_2)}}{4(\zeta_1 - \sigma_2)} + CT \tag{2.17} \\ \gamma_2 = & -\frac{\tilde{\zeta}_2B_2(\tau_1)^3e^{3i\zeta_1\tau_0}}{8\zeta_1^2} - \frac{e^{i\tau_0(\zeta_1+\sigma_2)}[\zeta_1^2\tilde{\zeta}_5B_1(\tau_1)B_2(\tau_1) + \zeta_1\zeta_4\sigma_2B_1(\tau_1)B_2(\tau_1)]}{\sigma_2(2\zeta_1 + \sigma_2)} \\ & + \frac{i\sigma_2\tilde{\zeta}_3B_1(\tau_1)e^{i\sigma_2\tau_0}}{(\sigma_2 - \zeta_1)(\zeta_1 + \sigma_2)} + \frac{e^{i\tau_0(\zeta_1-\sigma_2)}[\zeta_1^2\tilde{\zeta}_5B_2(\tau_1)\tilde{B}_1(\tau_1) - \zeta_1\zeta_4\sigma_2B_2(\tau_1)\tilde{B}_1(\tau_1)]}{\sigma_2(2\zeta_1 - \sigma_2)} + CT \end{aligned}$$

where CT represents the conjugates of the preceding terms.

2.3. Modulation equations

The modulation equations are a group of four first-order ODEs that describe the modulation of amplitudes and phases, since the procedures for solving them are complemented by initial conditions.

Secular terms in Eqs. (2.18) appear when the previous solutions are substituted into second-order Eqs (2.17). These terms act as conditions for solvability, which must be eliminated to obtain the modulation equations.

In order to eliminate the secular terms from the equations, we use a method that involves introducing new, unknown complex value functions that are defined in Eq. (2.19). These functions are then substituted into the secular terms. Canceling them effectively allows us to obtain the modulation equations. This, in turn, enables us to arrive at the final asymptotic solution. These secular terms in α_2 and γ_2 follow

$$\begin{aligned} \alpha_{2,s} = & -2\zeta_1^2B_1(\tau_1)B_2(\tau_1)\tilde{\sigma}_7(\tau_1)\tilde{B}_2(\tau_1) - 2i\sigma_2\frac{\partial B_1(\tau_1)}{\partial \tau_1} \\ \gamma_{2,s} = & 3\tilde{\zeta}_2B_2(\tau_1)^2\tilde{B}_2(\tau_1) - 2i\zeta_1\frac{\partial B_2(\tau_1)}{\partial \tau_1} \end{aligned} \tag{2.18}$$

and

$$B_k = \frac{1}{2}a_k(\tau)e^{i\psi_k} \quad \tilde{B}_k = \frac{1}{2}a_k(\tau)e^{-i\psi_k} \quad k = 1, 2 \tag{2.19}$$

where the order ψ_j and a_j represent the phases and amplitude of the solutions α and γ , respectively, for $j = 1, 2$.

Once we removed the secular terms from α_2 and γ_2 , we arrived at the ensuing modulation equations

$$\dot{a}_1(\tau) = 0 \quad \dot{a}_2(\tau) = 0 \quad \dot{\psi}_1(\tau) = \frac{\zeta_1^2a_2(\tau)^2\sigma_7}{4\sigma_2} \quad \dot{\psi}_2(\tau) = -\frac{3a_2(\tau)^2\zeta_2}{8\zeta_1} \tag{2.20}$$

Once we reconstituted the modulation equations for nonresonant cases and took into account established equations (2.20), we obtained the final asymptotic solution up to the second-order

approximations, with a_i and ψ_i being dependent on τ_1 for $i = 1, 2$. The resulting solution is as follows

$$\begin{aligned}
 \alpha = & \frac{a_2(\tau)^2(\zeta_1^2\sigma_6 + \sigma_3) - 2\sigma_1}{2\sigma_2^2} + a_1(\tau) \cos(\sigma_2\tau + \psi_1(\tau)) \\
 & + \frac{a_2(\tau)^2(\sigma_3 - \zeta_1^2\sigma_6) \cos[2(\zeta_1\tau + \psi_2(\tau))]}{8\zeta_1^2 - 2\sigma_2^2} - \frac{\sigma_5 a_1(\tau) a_2(\tau) \sin[\tau(\zeta_1 + \sigma_2) + \psi_1(\tau) + \psi_2(\tau)]}{2(\zeta_1 + 2\sigma_2)} \\
 & - \frac{\sigma_5 a_1(\tau) a_2(\tau) \sin[\tau(\zeta_1 - \sigma_2) - \psi_1(\tau) + \psi_2(\tau)]}{2(\zeta_1 - 2\sigma_2)} \\
 & - \frac{\zeta_1 \sigma_7 a_1(\tau) a_2(\tau)^2 \cos[\tau(2\zeta_1 + \sigma_2) + \psi_1(\tau) + 2\psi_2(\tau)]}{16(\zeta_1 + \sigma_2)} - \frac{\zeta_1 \sigma_4 a_2(\tau) \sin(\zeta_1\tau + \psi_2(\tau))}{\zeta_1^2 - \sigma_2^2} \\
 & - \frac{\zeta_1 \sigma_7 a_1(\tau) a_2(\tau)^2 \cos[\tau(2\zeta_1 - \sigma_2) - \psi_1(\tau) + 2\psi_2(\tau)]}{16(\zeta_1 - \sigma_2)} \\
 \gamma = & a_2(\tau) \cos(\zeta_1\tau + \psi_2(\tau)) + \frac{\zeta_1 a_1(\tau) a_2(\tau) (\zeta_1 \zeta_5 - \zeta_4 \sigma_2) \cos[\tau(\zeta_1 - \sigma_2) - \psi_1(\tau) + \psi_2(\tau)]}{2\sigma_2(2\zeta_1 - \sigma_2)} \\
 & - \frac{\zeta_1 a_1(\tau) a_2(\tau) (\zeta_1 \zeta_5 + \zeta_4 \sigma_2) \cos[\tau(\zeta_1 + \sigma_2) + \psi_1(\tau) + \psi_2(\tau)]}{2\sigma_2(2\zeta_1 + \sigma_2)} + \frac{\zeta_3 \sigma_2 a_1(\tau) \sin(\sigma_2\tau\psi_1(\tau))}{\zeta_1^2 - \sigma_2^2} \\
 & - \frac{\zeta_2 a_2(\tau)^3 \cos[3(\zeta_1\tau + \psi_2(\tau))]}{32\zeta_1^2}
 \end{aligned} \tag{2.21}$$

2.4. Comparison between analytical and numerical solutions using time histories

To compare the dimensionless form of equations of motion (2.9) with second-order asymptotic solution (2.21), we present a time history based on the data provided in Eqs. (2.22).

In Figs. 2a,b, we depict the time histories for two degrees of freedom of the dynamical system, namely, $x(\tau)$ and $\phi_1(\tau)$, respectively. It is noteworthy that both the analytical and numerical solutions demonstrate satisfactory accuracy of the obtained approximation. Hence, even a simplified model of the dynamical system can be efficiently solved analytically using the presented approach.

$$\begin{aligned}
 \sigma_1 = 0.0025 & \quad \sigma_2 = 1.01 & \quad \sigma_3 = 0.06 & \quad \sigma_4 = 0.014 \\
 \sigma_5 = 0.06 & \quad \sigma_6 = 0.01 & \quad \sigma_7 = 0.05 & \quad \zeta_1 = 1.0 \\
 \zeta_2 = 0.1667 & \quad \zeta_3 = 0.0005 & \quad \zeta_4 = 0.01 & \quad \zeta_5 = 0.005 \\
 x(\tau) = 0.04 & \quad \dot{x}(\tau) = 0 & \quad \phi(\tau) = 0.01 & \quad \dot{\phi}(\tau) = 0
 \end{aligned} \tag{2.22}$$

The obtained solutions are then compared by plotting them in time history plots. The masses of pendulums and length of the string greatly influence the simulation results. Furthermore, these results can be utilized to gain more insights into energy transfers, tension in the string, and other critical characteristics of the system.

2.4.1. Compliance error

To ensure solution dependability and precision, time histories of compliance errors in the results are presented. This not only aids potential computation optimization but also contributes to advancing numerical methods. These histories, integrated with the results, enhance visualization of discrepancies in individual time intervals. Additionally, the Root Mean Square Error (RMSE) and Mean Absolute Error (MAE) are computed using $\sum_{n=1}^N [Num_i - Apr_i]^2/n$ and $\sum_{n=1}^N [|Num_i - Apr_i|]/n$, respectively. Here, Num is the numerical solution, Apr is the approximate solution, and N is the number of observations. These metrics provide additional tools

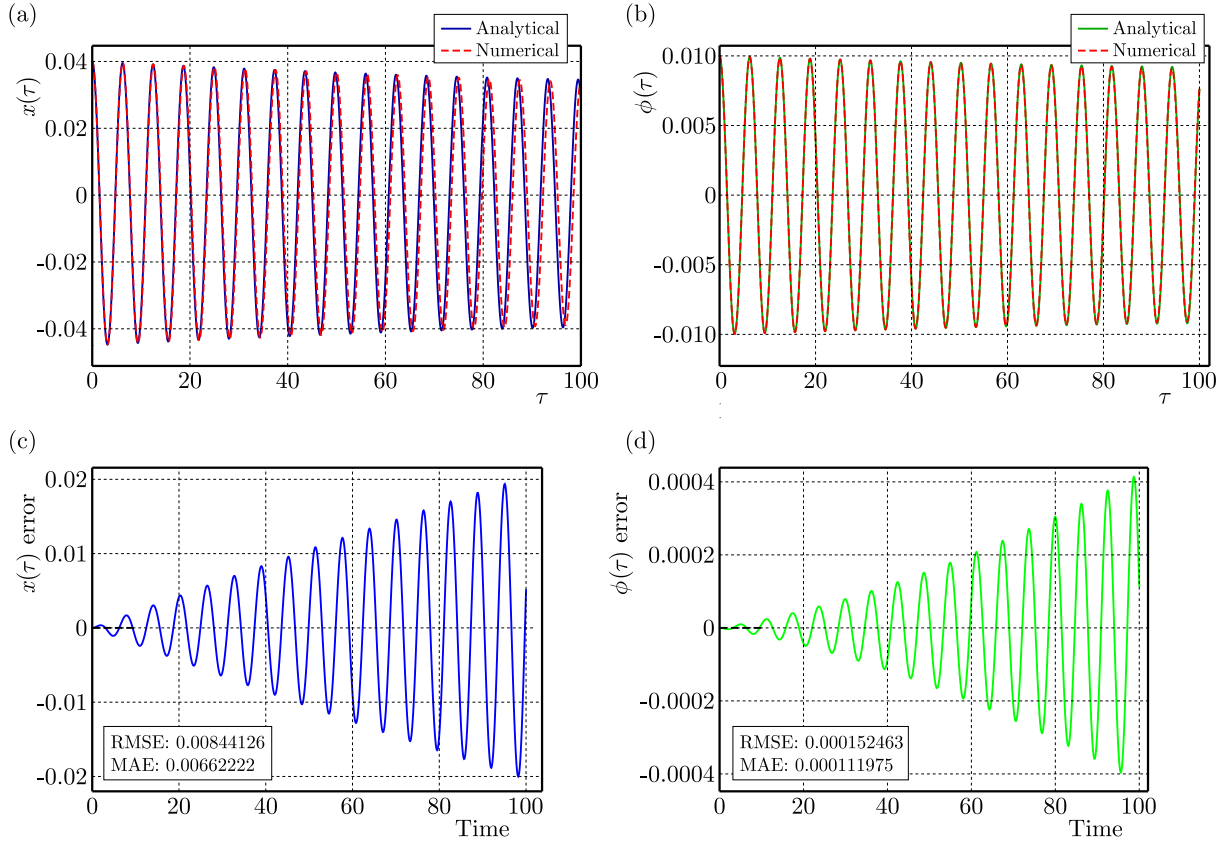


Fig. 2. (a) Comparison between the analytical (in blue, Eq. (2.9)₁) and numerical (in red, Eq. (2.21)₁) solution using the parameters given in Eqs. (2.22). (b) Comparison between analytical ($\phi(\tau)$ in green, Eq. (2.9)₂) and numerical (β in red, Eq. (2.21)₂) solution using the parameters presented in Eqs. (2.22). (c) Compliance error for $x(\tau)$ with RMSE = 0.00844126 and MAE = 0.00662222. (d) Compliance error for $\phi(\tau)$ with RMSE = 0.000152463 and MAE = 0.00011975

for a thorough assessment of solution accuracy, offering a more comprehensive understanding of overall performance.

Figures 2c and 2d depict the deviation between numerical and approximate solutions along the x -axis (representing time). The y -axis shows the compliance error at each point. Peaks or shifts in error plots signify notable deviations between solutions, while a declining trend suggests convergence of the numerical solution. Oscillations in the compliance errors indicate sensitivity to parameters and initial conditions. RMSE and MAE values are very small, affirming improved performance of the method and appropriateness of the dataset.

Moving forward to the next Section, we show a more advanced version of the variable-length pendulum with 4-DOF. The process used to obtain the solutions for this system closely mirrors the one employed earlier, encompassing all the fundamental assumptions and culminating in generating and comparing the results in time history plots.

3. The original modification of SAM

We introduce a novel and innovative modification to the SAM model based on the work presented in (Yakubu *et al.*, 2022). This modified version demonstrates potentially richer dynamics, as depicted in Fig. 1b. To achieve this, we have added a second spring pendulum to the non-swinging mass M , on the opposite end. The two pendulums, with masses of m_1 and m_2 , are connected by a suspension configuration with a stiffness k and a damper c . Point 0_2 is free to rotate and

subject to oscillation in the (X, Y) plane, while point O_1 is fixed, allowing for the variability of length l_1 and the double pendulum configurations. The distance of l_2O is measured between the two pendulums, and l_2 denotes the extension caused by the spring between them. The original Modified SAM model can be applied to various scenarios, including wave variability, suspension systems, elastic robotic links, and load-lifting equipment such as cranes. $X_0 = f_0 \sin(\omega t + \theta)$ is a time function that represents the periodic kinematic excitation. The displacement is measured from the origin of the coordinate system O specifically in the direction of the x -axis. Here, f_0 is the excitation force, ω and θ represent the angular frequency and phase shift of the excitation, respectively, while s denotes the distance in the X direction from the point O to the fixed support point O_1 .

3.1. Equations of motion

The equation of motion for the 4-DOF MSAM model is derived in (Yakubu *et al.*, 2022) using Newton's second law and the Lagrangian mechanics. The system equations of motion, when friction in pulley bearing is neglected, are

$$\begin{aligned}
 \ddot{l}_1 &= \frac{1}{m_1 + M} [T_2 \cos(\varphi_2 - \varphi_1) - (M + m_1 \sin \varphi_1) \ddot{X}_0 + m_1(l_1 \dot{\varphi}_1^2 + g \cos \varphi_1) - Mg] \\
 \ddot{l}_2 &= \frac{1}{2m_1 m_2 (m_1 + M)} \left(\{M m_1 T_2 [\cos(2(\varphi_2 - \varphi_1))] - 1\} M m_1 m_2 \{ \ddot{X}_0 [2 \cos(\varphi_2 - \varphi_1) \right. \\
 &\quad \left. + \sin(\varphi_2 - 2\varphi_1) - \sin \varphi_2] + g \} + 2m_1 m_2 [M l_1 \dot{\varphi}_1^2 \cos(\varphi_2 - \varphi_1) + (m_1 + M)(l_1 + l_{20}) \dot{\varphi}_2^2] \right. \\
 &\quad \left. - 2m_1 T_2 (m_1 + m_2 + M) \right) \\
 \ddot{\varphi}_1 &= \frac{T_2 \sin(\varphi_2 - \varphi_1) - m_1 (2\dot{l}_1 \dot{\varphi}_1 + \ddot{X}_0 \cos \varphi_1 + g \sin \varphi_1)}{m_1 l_1} \\
 \ddot{\varphi}_2 &= \frac{1}{2(m_1^2 + M m_1)(l_2 + l_{20})} \left\{ [-M T_2 \sin(2(\varphi_2 - \varphi_1)) - M g m_1 (2 \sin(\varphi_2 - \varphi_1)) \right. \\
 &\quad \left. + \sin(\varphi_2 - 2\varphi_1) + \sin \varphi_2] - M m_1 \ddot{X}_0 [2 \sin(\varphi_2 - \varphi_1) - \cos(\varphi_2 - 2\varphi_1) + \cos \varphi_2] \right. \\
 &\quad \left. - 2M m_1 l_1 \dot{\varphi}_1^2 \sin(\varphi_2 - \varphi_1) - 4m_1 \dot{l}_2 \dot{\varphi}_2 (m_1 + M) \right\}
 \end{aligned} \tag{3.1}$$

where $T_2 = (cl_2 + kl_2)$ and $l_1, l_2, \varphi_1, \varphi_2$ are t dependent variables.

Besides the assumptions outlined in Section 1.1, it is worth noting that the length l_1 exhibits motion opposite to that of l_2 . Thus, to transform the system to a solvable form using the multiple scale method, we introduce dimensionless parameters presented in Appendix A.1 to adhere to the system investigational process.

$x_1(\tau), x_2(\tau), \phi_1(\tau)$ and $\phi_2(\tau)$ are dimensionless forms of $l_1(t), l_2(t), \varphi_1(t)$ and $\varphi_2(t)$, respectively. ω_1 is first associated with $\dot{\phi}_1(\tau)$, then λ is introduced into both $x_1(\tau)$ and $\dot{\phi}_1(\tau)$ for the same reasons stated in Section 2.1. Additionally, we employ the following approximation based on the Taylor series. In this approximation, we retain only the first term of Taylor's expansion, which can be expressed as follows

$$\begin{aligned}
 \sin \phi_i(t) &= \phi_i(t) - \frac{(\phi_i(t))^3}{6} & \cos \phi_i &= 1 - \frac{(\phi_i(t))^2}{2} \\
 \sin[2(\phi_{i+1}(t) - \phi_i(t))] &= 2[\phi_{i+1}(t) - \phi_i(t)] & \cos[2(\phi_{i+1}(t) - \phi_i(t))] &= 1 \\
 \sin(\phi_{i+1}(t) - \phi_i(t)) &= \phi_{i+1}(t) - \phi_i(t) & \cos(\phi_{i+1}(t) - \phi_i(t)) &= 1 \\
 \sin(\phi_{i+1}(t) - 2\phi_i(t)) &= \phi_{i+1}(t) - 2\phi_i(t) & \cos(\phi_{i+1}(t) - 2\phi_i(t)) &= 1
 \end{aligned} \tag{3.2}$$

Using the parameters in Appendix A.1, then the final dimensionless form of Eqs. (3.1) can be written as it is presented in Appendix A.2.

3.2. The multiple scale method

Our analysis concentrates on a small region near the system static equilibrium. To characterize the amplitudes of the oscillations within this region, we use a small parameter, denoted by $0 < \varepsilon \ll 1$

$$\begin{aligned} x_1(\tau) &= \varepsilon\alpha(\tau : \varepsilon) & x_2(\tau) &= \varepsilon\beta(\tau : \varepsilon) \\ \phi_1(\tau) &= \varepsilon\gamma(\tau : \varepsilon) & \phi_2(\tau) &= \varepsilon\Gamma(\tau : \varepsilon) \end{aligned} \quad (3.3)$$

By assuming a small area around the system static equilibrium position and the amplitude of oscillations within that area, as is consistent with the MSM, we can make the following approximations (Abohamer *et al.*, 2023a; Awrejcewicz *et al.*, 2022)

$$\begin{aligned} b &= \varepsilon\tilde{b} & F &= \varepsilon\tilde{F} & c_1 &= \varepsilon\tilde{c}_1 & G_2 &= \varepsilon\tilde{G}_2 & \omega_0 &= \varepsilon\tilde{\omega}_0 \\ \sigma_1 &= \varepsilon^2\tilde{\sigma}_1 & \sigma_2 &= \varepsilon^2\tilde{\sigma}_2 & \sigma_3 &= \varepsilon\tilde{\sigma}_3 & \sigma_4 &= \varepsilon^{-1}\tilde{\sigma}_4 & \sigma_6 &= \varepsilon\tilde{\sigma}_6 \\ \sigma_9 &= \varepsilon^{-1}\tilde{\sigma}_9 & A &= \varepsilon\tilde{A} & b_2 &= \varepsilon\tilde{b}_2 & b_3 &= \varepsilon\tilde{b}_3 & G &= \varepsilon^{-1}\tilde{G} \\ G_1 &= \varepsilon^{-1}\tilde{G}_1 & \delta_2 &= \varepsilon\tilde{\delta}_2 & \delta_3 &= \varepsilon\tilde{\delta}_3 & \delta_5 &= \varepsilon^{-1}\tilde{\delta}_5 & \delta_7 &= \varepsilon\tilde{\delta}_7 \\ \delta_8 &= \varepsilon\tilde{\delta}_8 & \delta_9 &= \varepsilon\tilde{\delta}_9 & \delta_1 &= \varepsilon^2\tilde{\delta}_1 & y &= \varepsilon\tilde{y} & c_2 &= \varepsilon\tilde{c}_2 \\ \zeta_3 &= \varepsilon\tilde{\zeta}_3 & \zeta_2 &= \varepsilon^{-1}\tilde{\zeta}_2 & h &= \varepsilon^{-1}\tilde{h} & \xi_1 &= \varepsilon\tilde{\xi}_1 & \xi_6 &= \varepsilon^{-1}\tilde{\xi}_6 \\ \xi_9 &= \varepsilon^{-1}\tilde{\xi}_9 & \xi_{10} &= \varepsilon^{-1}\tilde{\xi}_{10} & \xi_{11} &= \varepsilon^{-2}\tilde{\xi}_{11} \end{aligned} \quad (3.4)$$

In line with the methodology of the multiple scale approach, the time-dependent variables $x_1(\tau)$, $x_2(\tau)$, $\phi_1(\tau)$ and $\phi_2(\tau)$ can be considered as power series of ε

$$\begin{aligned} x_1(\tau) &= \sum_{k=1}^2 \varepsilon^k x_{1,k}(\tau_0, \tau_1) + O(\varepsilon^k) & x_2(\tau) &= \sum_{k=1}^2 \varepsilon^k x_{2,k}(\tau_0, \tau_1) + O(\varepsilon^k) \\ \phi_1(\tau) &= \sum_{k=1}^2 \varepsilon^k \phi_{1,k}(\tau_0, \tau_1) + O(\varepsilon^k) & \phi_2(\tau) &= \sum_{k=1}^2 \varepsilon^k \phi_{2,k}(\tau_0, \tau_1) + O(\varepsilon^k) \end{aligned} \quad (3.5)$$

It is worth emphasizing that these operators exclude terms of $O(\varepsilon^2)$ and higher orders. To derive the PDE groups associated with different powers of ε , we substitute Eqs. (3.3)-(3.5) into the dimensionless form of governing equations (A.2) in Appendix. This process involves a splitting method based on the perturbation parameter ε (Awrejcewicz *et al.*, 2022). Then, we derive the preceding 8 linear PDEs, each corresponding to a specific order of ε and ε^2 :

— first-order equations (coefficient 1 at ε^1)

$$\frac{\partial^2 \alpha_1}{\partial \tau_0^2} + w^2 \alpha_1 = 0 \quad \frac{\partial^2 \beta_1}{\partial \tau_0^2} + \beta_1 = 0 \quad \frac{\partial^2 \gamma_1}{\partial \tau_0^2} + \omega_4^2 \gamma_1 = 0 \quad \frac{\partial^2 \Gamma_1}{\partial \tau_0^2} + \xi_4^2 \Gamma_1 = 0 \quad (3.6)$$

— second-order equations (coefficient 2 at ε^2) (refer to Appendix A.3) where α_1 , β_1 , γ_1 , Γ_1 represent the solutions of the first-order approximations of the time-dependent variables $x_1(\tau)$, $x_2(\tau)$, $\phi_1(\tau)$, $\phi_2(\tau)$, respectively. Also, α_2 , β_2 , γ_2 , Γ_2 are the solutions of the second-order approximations of the time-dependent variables $x_1(\tau)$, $x_2(\tau)$, $\phi_1(\tau)$, $\phi_2(\tau)$. Meanwhile, the general solutions of the time-dependent variables will be represented by α , β , γ , and Γ , respectively.

The solutions to obtained Eqs. (a.3) in Appendix, which can be solved in a particular sequence, emphasize the importance of the solutions in the first category. Thus, our primary focus is on obtaining the general solutions to Eqs. (3.6). The solutions obtained are as follows

$$\begin{aligned} \alpha_1 &= e^{iw\tau_0} B_1(\tau_1) + e^{-iw\tau_0} \tilde{B}_1(\tau_1) & \beta_1 &= e^{i\tau_0} B_2(\tau_1) + e^{-i\tau_0} \tilde{B}_2(\tau_1) \\ \gamma_1 &= e^{i\omega_4\tau_0} B_3(\tau_1) + e^{-i\omega_4\tau_0} \tilde{B}_3(\tau_1) & \Gamma_1 &= e^{i\xi_4\tau_0} B_4(\tau_1) + e^{-i\xi_4\tau_0} \tilde{B}_4(\tau_1) \end{aligned} \quad (3.7)$$

As a result, by substituting solutions (3.7) into the second group of PDEs (A.3) in Appendix, we derive the 2-order solutions as α_2 , β_2 , γ_2 and Γ_2 , where B_i and \tilde{B}_i depend on τ_1 , i takes values of $1, \dots, 4$.

3.3. Modulation equations

The modulation equations constitute a set of eight first-order ODEs describing the amplitude and phase modulation. These equations necessitate initial conditions for the effective solution, which complement the solving procedures.

Secular terms, as observed in Eqs. (3.8), emerge when inserting the previously derived solutions into the second-order equations (refer to Eqs. (A.3) in Appendix). While serving as solvability conditions, these secular terms must be eliminated to obtain the modulation equations.

To eliminate the secular terms (see Eqs. (3.8)), we employ a method introducing new complex-valued functions, defined in Eqs. (3.9). Substituting these functions into the secular terms eliminates them, allowing derivation of the modulation equations. The final asymptotic solution is then obtained through these equations. The secular terms in α_2 , β_2 , γ_2 and Γ_2 are expressed as

$$\begin{aligned} \alpha_{2,s} &= -2\omega_4^2 \tilde{\sigma}_9 B_1(\tau_1) B_3(\tau_1) \tilde{B}_3(\tau_1) - 2iw \frac{\partial B_1(\tau_1)}{\partial \tau_1} \\ \beta_{2,s} &= -\tilde{b}_2 B_2(\tau_1) - \tilde{b}_3 B_2(\tau_1) + 2\xi 4^2 \tilde{G} B_2(\tau_1) B_4(\tau_1) \tilde{B}_4(\tau_1) - 2i \frac{\partial B_2(\tau_1)}{\partial \tau_1} \\ &\quad + 2\xi 4^2 \tilde{G}_1 B_2(\tau_1) B_4(\tau_1) \tilde{B}_4(\tau_1) - i\tilde{c}_1 B_2(\tau_1) - i\tilde{\delta}_7 B_2(\tau_1) - i\tilde{\delta}_8 B_2(\tau_1) \\ \gamma_{2,s} &= 3\tilde{\zeta}_2 B_3(\tau_1)^2 \tilde{B}_3(\tau_1) - 2i\omega_4 \frac{\partial B_3(\tau_1)}{\partial \tau_1} \\ \Gamma_{2,s} &= -2\omega_4^2 \tilde{\xi}_{10} B_3(\tau_1) B_4(\tau_1) \tilde{B}_3(\tau_1) - 3\tilde{\xi}_6 B_4(\tau_1)^2 \tilde{B}_4(\tau_1) - 2i\xi_4 \frac{\partial B_4(\tau_1)}{\partial \tau_1} \end{aligned} \tag{3.8}$$

and

$$B_j = \frac{1}{2} a_j(\tau) e^{i\psi_j(\tau_1)} \quad \tilde{B}_j = \frac{1}{2} a_j(\tau) e^{-i\psi_j(\tau_1)} \tag{3.9}$$

where ψ_j and a_j represent the phases and amplitude of the solutions α , β , γ , and Γ , respectively. For $j = 1, 2, 3, 4$.

After eliminating the secular terms from α_2 , β_2 , γ_2 and Γ_2 , the modulation equations are obtained as

$$\begin{aligned} \dot{a}_1(\tau) &= 0 & \dot{a}_3(\tau) &= 0 & \dot{\psi}_1(\tau) &= \frac{\omega_4^2 a_3(\tau)^2 \sigma_9}{4w} \\ \dot{\psi}_3(\tau) &= -\frac{3a_3(\tau)^2 \zeta_2}{8\omega_4} & \dot{a}_2(\tau) &= -\frac{1}{2} a_2(\tau) (c_1 + \delta_7 + \delta_8) & \dot{a}_4(\tau) &= 0 \\ \dot{\psi}_2(\tau) &= \frac{1}{4} [2b_2 + 2b_3 + \xi_4^2 a_4(\tau)^2 (G + G_1)] & \dot{\psi}_4(\tau) &= \frac{2\omega_4^2 a_3(\tau)^2 \xi_{10} + 3a_4(\tau)^2 \xi_6}{8\xi_4} \end{aligned} \tag{3.10}$$

After reconstituting the modulation equations for nonresonant cases and considering the equations established in Eq. (3.7), the final asymptotic solution up to the second-order approximation for α , β , γ and Γ , with a_i and ψ_i being dependent on τ_1 , where $i = 1, 2, 3, 4$, have been obtained.

3.4. Comparison between analytical and numerical solutions using time histories

For comparison, the dimensionless form of the equations of motion (see Eqs. (A.1) and (A.2) in Appendix) and the asymptotic solution up to the second-order approximation are shown in

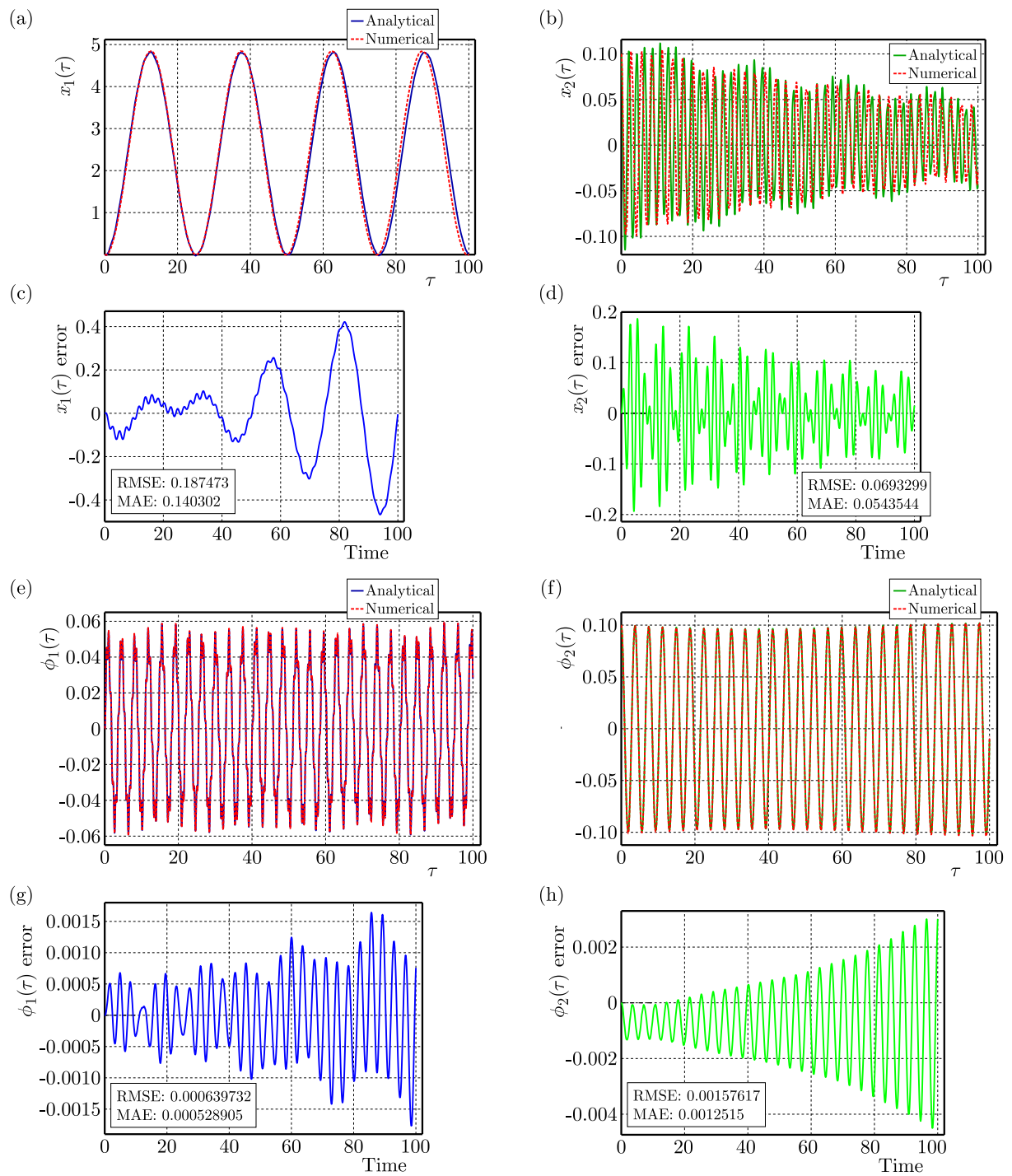


Fig. 3. (a) Comparison between analytical (in blue) and numerical (in red) solutions using the parameters presented in Eq. (3.11). (b) Comparison between analytical (in green) and numerical (in red) solutions using the parameters presented in Eq. (3.11). (c) Compliance error for $x_1(\tau)$ with RMSE = 0.187473 and MAE = 0.140302. (d) Compliance error for $x_2(\tau)$ with RMSE = 0.0693299 and MAE = 0.0543544. (e) Comparison between analytical (in blue) and numerical (in red) solutions using the parameters presented in Eq. (3.11). (f) Comparison between analytical (in green) and numerical (in red) solutions using the parameters presented in Eq. (3.11). (g) Compliance error for $\phi_1(\tau)$ with RMSE = 0.000639732 and MAE = 0.000528905. (h) Compliance error for $\phi_2(\tau)$ with RMSE = 0.00157617 and MAE = 0.0012515

the time history using the data in below. All initial conditions, except for $x_2(0) = \phi_2(0) = 0.1$, are set to zero

$$\begin{aligned}
 A &= 0.5 & c_1 = c_2 = \xi_1 = \xi_3 = \delta_3 &= 0.01 & \sigma_5 = \zeta_3 &= 0.0001 & \xi_4 &= 1.61 \\
 \omega_5 = \xi_2 &= 0.002 & \sigma_6 = \sigma_7 = \xi_{10} = \xi_{11} &= 0.0002 & \sigma_8 &= 0.0004 & & \\
 \xi_{12} &= 0.00004 & \xi_5 = 0.005 & \sigma_9 = \xi_{14} = \zeta_4 &= 0.00005 & \delta_2 &= 0.001 & \\
 \delta_4 &= 0.003 & \delta_5 = 0.00008 & \xi_7 = 0.0012 & h = \omega_0 &= 1 & & \\
 \delta_8 &= 0.008 & \delta_9 = 0.00009 & \delta_0 = 0.00002 & \xi_6 &= 0.00008 & & \\
 \xi_9 &= 0.000021 & \omega = 10 & \xi_{13} = 0.00015 & \sigma_1 &= 0.15 & & \\
 \sigma_2 &= 0.464 & b_2 = 2.11 & b_3 = 1.63 & G = 0.8 & G_1 &= 0.1 & \\
 F &= 0.81 & \omega_4 = 1.72 & \zeta_1 = 0.05 & \sigma_3 = 1.15 & w &= 0.25 &
 \end{aligned} \tag{3.11}$$

Figure 3a, 3b, 3e and 3f represent the time history for $x_1(\tau)$, $x_2(\tau)$, $\phi_1(\tau)$ and $\phi_2(\tau)$, respectively. As we can observe, both the analytical and numerical solutions indicate the accuracy of the system equation. Figure 3c, 3d, 3g and 3h depicts the deviation between the numerical and approximate solutions for $x_1(\tau)$, $x_2(\tau)$, $\phi_1(\tau)$ and $\phi_2(\tau)$, respectively. The compliance error for the modified SAM follows the same trend as that of the SAM. Therefore, it aligns with the presumption stated in Section 2.4.1. It becomes evident that the 4-DOF system can be effectively solved analytically by employing the multiple scale approach. However, it comes with a drawback in that it offers an approximate solution, and its accuracy depends on the number of time scales used. As a result, it becomes crucial to identify particular traits between the analytical and numerical solutions to compare them accurately and guarantee their correctness.

4. Conclusions

This publication focuses on the modeling and analysis challenges posed by variable-length pendulums, with a particular emphasis on the 4-DOF system. The attainment of an analytical solution not only validates the model but also contributes to improved efficiency, accuracy, and theoretical advancements. These analytical solutions serve as crucial tools for the investigation of dynamical systems, finding applications across diverse scientific and engineering fields. Furthermore, the study identifies promising directions for future research, urging exploration into steady-state solutions and conducting thorough stability analyses.

The publication highlights the practical applications of the analyzed models, revealing their potential in studying dynamic entities like robots and load-lifting devices. For instance, the study suggests examining a system comprising three inverted pendulums to represent different segments of the human body or analyzing the dynamics of load-lifting devices such as cranes. This approach extends the utility of the findings, offering insights into a broader applicability of the studied parametric dynamical models. Notably, the potential application of these insights in the field of energy harvesting is also underscored, adding a dimension of practical significance to the theoretical advancements presented in the publication.

A. Appendix

A.1. Dimensionless parameters for the modified SAM

$$A = \frac{l_{20}}{l} \quad G = \frac{M}{(m_1 + M)} \quad G_1 = \frac{m_1}{(m_1 + M)} \quad \omega_2^2 = \frac{g}{l} \quad \omega_3^2 = \frac{k}{m_1}$$

$$\begin{aligned}
\omega_1^2 &= \frac{k}{m_1 + M} & \lambda^2 &= \frac{\omega_1^2 \omega_1}{G_1} & c_1 &= \frac{c}{(m_1 + M)\omega_1} & F &= \frac{f_0 \omega^2}{l \omega_1^2} \\
c_2 &= \frac{c}{\lambda \omega_1} & b_1 &= \frac{M}{m_1} & b_2 &= \frac{M}{m_2} & b_3 &= \frac{m_1}{m_2} & \omega_4^2 &= \frac{\omega_2^2}{\omega_1^2} \\
\omega_5^2 &= \frac{\omega_3^2}{\lambda \omega_1^2} & \sigma_1 &= \omega^2 \lambda + G \omega_4^2 - \frac{\omega^2 \omega_1^2 \omega_4^2}{\lambda^2} & \sigma_2 &= FG & \sigma_3 &= \frac{F \omega^2 \omega_1^2}{\lambda^2} \\
\sigma_4 &= \frac{F \omega^2 \omega_1^2}{6 \lambda^2} & \sigma_5 &= \frac{\omega^2 \omega_1^2 \omega_4^2}{2 \lambda^2} & \sigma_6 &= \omega^2 \omega_1 & \sigma_7 &= \frac{\omega^2 \omega_1^2}{\lambda} \\
\sigma_8 &= \frac{2 \omega^2 \omega_1^2}{\lambda} & \sigma_9 &= \frac{\omega^2 \omega_1^2}{\lambda^2} & \delta_0 &= G \lambda & \delta_1 &= \frac{G \lambda^3}{\omega_1^2} + \frac{5 G \omega_4^2}{2} \\
\delta_2 &= \frac{G \lambda^2}{\omega_1^2} & \delta_3 &= FG \omega_0 & \delta_4 &= \frac{G \omega_4^2}{4} & \delta_5 &= \frac{FG}{12} & \delta_6 &= \frac{2 G \lambda}{\omega_1} \\
\delta_7 &= b_2 c_1 & \delta_8 &= b_3 c_1 & \delta_9 &= \frac{2 G \lambda^2}{\omega_1} & \zeta_1 &= \frac{F}{3} + \frac{5 G \omega_4^2}{2} \\
\zeta_2 &= \frac{\omega_4^2}{6} & \zeta_3 &= \frac{2}{\omega_1} & \zeta_4 &= \frac{1}{\lambda} & \xi_1 &= \frac{G \lambda^3}{A \omega_1^2} + 2 G \omega_4^2 \\
\xi_2 &= \frac{G \lambda^2}{A \omega_1^2} & \xi_3 &= G \omega_5^2 & \xi_4 &= \frac{G \lambda^3}{A \omega_1^2} + G \omega_4^2 & \xi_5 &= \frac{h F G}{4} \\
\xi_6 &= \frac{G \omega_4^2}{12} & h &= 1 & \xi_7 &= c_2 G & \xi_8 &= \frac{2 G \lambda^2}{A \omega_1} & x i_9 &= \frac{2 G \lambda}{A \omega_1} \\
\xi_{10} &= \frac{G \lambda}{A} & \xi_{11} &= \frac{G}{A} & \xi_{12} &= \frac{2 G}{A} & \xi_{13} &= \frac{2 G_1}{A} & \xi_{14} &= \frac{1}{A}
\end{aligned} \tag{A.1}$$

A.2. The final dimensionless form of the modified SAM equations of motion

$$\begin{aligned}
& \sigma_1 - \sigma_2 \sin(\bar{\omega} \tau) - \omega^2 x_1(\tau) - \omega_0 x_2(\tau) - \sigma_3 \sin(\bar{\omega} \tau) \phi_1(\tau) + \sigma_4 \sin(\bar{\omega} \tau) \phi_1^3(\tau) + \sigma_5 \phi_2^2(\tau) \\
& \quad - c_1 \dot{x}_2(\tau) - \sigma_6 \phi_1(\tau) - \sigma_7 \dot{\phi}_1^2(\tau) - \sigma_8 x_1(\tau) \dot{\phi}_1(\tau) - \sigma_9 x_1(\tau) \dot{\phi}_1^2(\tau) - \ddot{x}_1(\tau) = 0 \\
& \delta_1 - \sigma_2 \sin(\bar{\omega} \tau) + \delta_2 x_1(\tau) - x_2(\tau) - b_2 x_2(\tau) - b_2 x_2(\tau) - b_3 x_2(\tau) + \delta_3 \sin(\bar{\omega} \tau) \phi_1(\tau) \\
& \quad - \delta_4 \phi_2^2(\tau) - \delta_5 \sin(\bar{\omega} \tau) \phi_2^3(\tau) - c_1 \dot{x}_2(\tau) - \delta_7 \dot{x}_2(\tau) - \delta_8 \dot{x}_2(\tau) + \delta_9 \dot{\phi}_1(\tau) \\
& \quad + \delta_6 x_1(\tau) \dot{\phi}_1(\tau) + \delta_0 \dot{\phi}_1^2(\tau) + G x_1(\tau) \dot{\phi}_1^2(\tau) + \frac{1}{2} A G(\tau) \dot{\phi}_2^2(\tau) + A G_1(\tau) \dot{\phi}_2^2(\tau) \\
& \quad + G_1 x_2(\tau) \dot{\phi}_2^2(\tau) - \ddot{x}_2(\tau) = 0 \\
& F \sin(\bar{\omega} \tau) - \omega_4^2 \phi_1 + \omega_5^2 x_2(\tau) \phi_1(\tau) + \zeta_1 \phi_1^3(\tau) - \zeta_1 \sin(\bar{\omega} \tau) \phi_1^2(\tau) - \omega_5^2 x_2(\tau) \phi_2(\tau) \\
& \quad - \zeta_3 \dot{x}_1(\tau) - c_2 \phi_1(\tau) \dot{x}_2(\tau) + c_2 \phi_2(\tau) - \dot{x}_2(\tau) - 2 \zeta_4 \dot{x}_1(\tau) \dot{\phi}_1(\tau) - \zeta_4 x_1(\tau) \ddot{\phi}_1(\tau) \\
& \quad - \ddot{\phi}_1(\tau) = 0 \\
& \xi_1 \phi_1(\tau) + h \sigma_2 \sin(\bar{\omega} \tau) \phi_1(\tau) + \xi_2 x_1(\tau) \phi_1(\tau) + \xi_3 x_1(\tau) \phi_1(\tau) - \xi_4^2 \phi_2(\tau) - h \sigma_2 \sin(\bar{\omega} \tau) \phi_2(\tau) \\
& \quad - \xi_2 x_1(\tau) \phi_2(\tau) - \xi_3 x_2(\tau) \phi_2(\tau) - \xi_5 \sin(\bar{\omega} \tau) \phi_2^2(\tau) - \xi_6 \phi_2^3(\tau) + \xi_7 \phi_1(\tau) \dot{x}_2(\tau) \\
& \quad - \xi_7 \phi_2(\tau) \dot{x}_2(\tau) + \xi_8 \phi_1(\tau) \dot{\phi}_2^2(\tau) + \xi_9 x_1(\tau) \phi_1(\tau) \dot{\phi}_2^2(\tau) - \xi_8 \phi_2(\tau) \dot{\phi}_1^2(\tau) \\
& \quad - \xi_9 x_1(\tau) \phi_2(\tau) \dot{\phi}_1^2(\tau) + \xi_{10} \phi_1(\tau) \dot{\phi}_1^2(\tau) \xi_{11} x_1(\tau) \phi_1(\tau) \dot{\phi}_1^2(\tau) - \xi_{10} \phi_2(\tau) \dot{\phi}_1^2(\tau) \\
& \quad - \xi_{11} x_1(\tau) \phi_2(\tau) \dot{\phi}_1^2(\tau) + \xi_{12} \dot{x}_2(\tau) \dot{\phi}_2^2(\tau) + \xi_{13} \dot{x}_2(\tau) \dot{\phi}_2^2(\tau) - \xi_{14} x_2(\tau) \ddot{\phi}_2(\tau) - \ddot{\phi}_2(\tau) = 0
\end{aligned} \tag{A.2}$$

A.3. Second-order equations of the modified SAM

$$\begin{aligned}
& \tilde{\sigma}_1 - \tilde{\sigma}_2 \sin(\omega\tau_0) - w^2\alpha_1 - \omega_0\beta_1 - \tilde{\sigma}_3\gamma_1 \sin(\omega\tau_0) + \tilde{\sigma}_4\gamma_1^3 \sin(\omega\tau_0) + \tilde{\sigma}_5\Gamma_1^2 \sin(\omega\tau_0) - \tilde{c}_1 \frac{\partial\beta_1}{\partial\tau_0} \\
& - \tilde{\sigma}_6 \frac{\partial\gamma_1}{\partial\tau_0} - \sigma_8\alpha_1 \frac{\partial\gamma_1}{\partial\tau_0} - \sigma_7 \left(\frac{\partial\gamma_1}{\partial\tau_0}\right)^2 - \tilde{\sigma}_6\alpha_1 \left(\frac{\partial\gamma_1}{\partial\tau_0}\right)^2 - 2\frac{\partial^2\alpha_1}{\partial\tau_0\partial\tau_1} - \frac{\partial^2\alpha_2}{\partial\tau_0^2} = 0 \\
& \tilde{\delta}_1 - \tilde{\delta}_2 \sin(\omega\tau_0) + \tilde{\delta}_2\alpha_1 - \tilde{b}_2\beta_1 - \tilde{b}_3\beta_1 - \beta_1 + \tilde{\delta}_3\gamma_1 \sin(\omega\tau_0) - \tilde{\delta}_4\Gamma_1^2 - \tilde{\delta}_5\Gamma_1^3 \sin(\omega\tau_0) - \tilde{c}_1 \frac{\partial\beta_1}{\partial\tau_0} \\
& - \tilde{\delta}_7 \frac{\partial\beta_1}{\partial\tau_0} - \tilde{\delta}_8 \frac{\partial\beta_1}{\partial\tau_0} + \tilde{\delta}_9 \frac{\partial\gamma_1}{\partial\tau_0} + \delta_6\alpha_1 \frac{\partial\gamma_1}{\partial\tau_0} + \delta_0 \left(\frac{\partial\gamma_1}{\partial\tau_0}\right)^2 + \tilde{G}\alpha_1 \left(\frac{\partial\gamma_1}{\partial\tau_0}\right)^2 + \frac{1}{2}\tilde{A}\tilde{G} \left(\frac{\partial\Gamma_1}{\partial\tau_0}\right)^2 \\
& + \tilde{A}\tilde{G}_1 \left(\frac{\partial\Gamma_1}{\partial\tau_0}\right)^2 + \tilde{G}\beta_1 \left(\frac{\partial\Gamma_1}{\partial\tau_0}\right)^2 + \tilde{G}_1\beta_1 \left(\frac{\partial\Gamma_1}{\partial\tau_0}\right)^2 - 2\frac{\partial^2\beta_1}{\partial\tau_0\partial\tau_1} - \frac{\partial^2\beta_2}{\partial\tau_0^2} = 0 \\
& \tilde{F} \sin(\omega\tau_0) + \omega_5^2\beta_1\gamma_1 - \zeta_1\gamma_1^2 \sin(\omega\tau_0) + \zeta_2\gamma_1^3 - \omega_4^2\gamma_2 - \omega_5^2\beta_1\Gamma_1 - \zeta_3 \frac{\partial\alpha_1}{\partial\tau_0} - 2\zeta_4 \frac{\partial\alpha_1}{\partial\tau_0} \frac{\partial\gamma_1}{\partial\tau_0} \quad (\text{A.3}) \\
& - 2\frac{\partial^2\gamma_1}{\partial\tau_0\partial\tau_1} - \zeta_4\alpha_1 \frac{\partial^2\gamma_1}{\partial\tau_0^2} - \frac{\partial^2\gamma_2}{\partial\tau_0^2} = 0 \\
& \tilde{\xi}_1\gamma_1 + \tilde{h}\tilde{\sigma}_2\gamma_1 \sin(\omega\tau_0) + \xi_2\alpha_1\gamma_1 + \xi_2\beta_1\gamma_1 - \tilde{h}\tilde{\sigma}_2\Gamma_1 \sin(\omega\tau_0) - \xi_2\alpha_1\Gamma_1 - \xi_3\beta_1\Gamma_1 \\
& - \xi_5\Gamma_1^2 \sin(\omega\tau_0) - \tilde{\xi}_6\Gamma_1^3 - \xi_4^2\Gamma_2 + \xi_7\gamma_1 \frac{\partial\beta_1}{\partial\tau_0} - \xi_7\Gamma_1 \frac{\partial\beta_1}{\partial\tau_0} + \xi_8\gamma_1 \frac{\partial\gamma_1}{\partial\tau_0} + \tilde{\xi}_9\alpha_1\gamma_1 \frac{\partial\gamma_1}{\partial\tau_0} \\
& - \xi_8\Gamma_1 \frac{\partial\gamma_1}{\partial\tau_0} - \tilde{\xi}_9\alpha_1\Gamma_1 \frac{\partial\gamma_1}{\partial\tau_0} + \tilde{\xi}_{10}\gamma_1 \left(\frac{\partial\gamma_1}{\partial\tau_0}\right)^2 + \tilde{\xi}_{11}\alpha_1\gamma_1 \left(\frac{\partial\gamma_1}{\partial\tau_0}\right)^2 - \tilde{\xi}_{10}\Gamma_1 \left(\frac{\partial\gamma_1}{\partial\tau_0}\right)^2 \\
& - \tilde{\xi}_{11}\alpha_1\Gamma_1 \left(\frac{\partial\gamma_1}{\partial\tau_0}\right)^2 + \xi_{12} \frac{\partial\beta_1}{\partial\tau_0} \frac{\partial\Gamma_1}{\partial\tau_0} + \xi_{13} \frac{\partial\beta_1}{\partial\tau_0} \frac{\partial\Gamma_1}{\partial\tau_0} - 2\frac{\partial\Gamma_1}{\partial\tau_0\partial\tau_1} - \xi_{14}\beta_1 \frac{\partial^2\Gamma_1}{\partial\tau_0^2} - \frac{\partial^2\Gamma_2}{\partial\tau_0^2} = 0
\end{aligned}$$

Acknowledgments

This research was funded by the National Center of Science (Narodowe Centrum Nauki) grant number 2019/35/B/ST8/00980 (NCN Poland). The authors contributed equally to this work.

References

1. ABADY I.M., AMER T.S., GAD H.M., BEK M.A., 2022, The asymptotic analysis and stability of 3DOF non-linear damped rigid body pendulum near resonance, *Ain Shams Engineering Journal*, **13**, 2, 101554
2. ABOHAMER M.K., AWREJCEWICZ J., AMER T.S., 2023a, Modeling and analysis of a piezoelectric transducer embedded in a nonlinear damped dynamical system, *Nonlinear Dynamics*, **31**, 1, 1-16
3. ABOHAMER M.K., AWREJCEWICZ J., AMER T.S., 2023b, Modeling of the vibration and stability of a dynamical system coupled with an energy harvesting device, *Alexandria Engineering Journal*, **63**, 377-397
4. AWREJCEWICZ J., STAROSTA R., SYPNIEWSKA-KAMIŃSKA G. (EDIT.), 2022, *Asymptotic Multiple Scale Method in Time Domain: Multi-Degree-of-Freedom Stationary and Nonstationary Dynamics*, 1st ed., Boca Raton, United States: Taylor and Francis Group
5. AWREJCEWICZ J., STAROSTA R., SYPNIEWSKA-KAMIŃSKA G., 2014, Asymptotic analysis and limiting phase trajectories in the dynamics of spring pendulum, [In:] *Applied Non-Linear Dynamical Systems*, Awrejcewicz J. (Ed.), Springer Proceedings in Mathematics and Statistics, Springer, Cham, vol. 93
6. CASASAYAS J., NUNES A., TUFILLARO N.B., 1990, Swinging Atwood's machine: integrability and dynamics, *Journal de Physique II*, **51**, 1693-1702

7. ELMANDOUH A.A., 2016, On the integrability of the motion of 3D-Swinging Atwood machine and related problems, *Physics Letters A*, **380**, 9, 989-991
8. MANAFIAN J., ALLAHVERDIYEVA N., 2022, An analytical analysis to solve the fractional differential equations, *Advanced Mathematical Models and Applications*, **6**, 2, 128-161
9. NAYFEH A.H., 2005, Resolving controversies in the application of the method of multiple scales and the generalized method of averaging, *Nonlinear Dynamics*, **40**, 61-102
10. NUNES A., CASASAYAS J., TUFILLARO N.B., 1995, Periodic orbits of the integrable swinging Atwood's machine, *American Journal of Physics*, **63**, 2, 121-126
11. PROKOPENYA A.N., 2017, Motion of a swinging Atwood's machine: simulation and analysis with Mathematica, *Mathematics in Computer Science*, **11**, 4, 417-425
12. PROKOPENYA A.N., 2021, Searching for equilibrium states of Atwood's machine with two oscillating bodies by means of computer algebra, *Programming and Computer Software*, **47**, 1, 43-49
13. PUJOL O., PÉREZ J.P., RAMIS J.P., SIMÓ C., SIMON S., WEIL J.A., 2010, Swinging Atwood machine: experimental and numerical results, and a theoretical study, *Physica D: Nonlinear Phenomena*, **239**, 12, 1067-1081
14. SEADAWY A.R., MANAFIAN J., 2018, New soliton solution to the longitudinal wave equation in a magneto-electro-elastic circular rod, *Results in Physics*, **8**, 1158-1167
15. STAROSTA R., SYPNIEWSKA-KAMIŃSKA G., AWREJCEWICZ J., 2017, Quantifying non-linear dynamics of mass-springs in series oscillators via asymptotic approach, *Mechanical Systems and Signal Processing*, **89**, 149-158
16. TUFILLARO N.B., 1985, Motions of a swinging Atwood's machine, *Journal de Physique*, **46**, 1495-1500
17. TUFILLARO N., 1986, Integrable motion of a swinging Atwood's machine, *American Journal of Physics*, **54**, 142-143
18. TUFILLARO N.B., 1988, Teardrop and heart orbits of a swinging Atwood's machine, *American Journal of Physics*, **62**, 3, 231-233
19. TUFILLARO N.B., NUNES A., CASASAYAS J., 1998, Unbounded orbits of a swinging Atwood's machine, *American Journal of Physics*, **56**, 1117-1120
20. YAKUBU G., OLEJNIK P., AWREJCEWICZ J., 2022, On the modeling and simulation of variable-length pendulum systems: A review, *Archives of Computational Methods in Engineering*, **29**, 4, 2397-2415
21. YEHA H.M., 2006, On the integrability of the motion of a heavy particle on a tilted cone and the swinging Atwood's machine, *Mechanics Research Communications*, **33**, 5, 711-716

Manuscript received November 12, 2023; accepted for print January 29, 2024